Pergamon

Cement and Concrete Research 29 (1999) 369–375

CEMENT AND CONCRETE RESEARCH

Microstructural features of concrete in relation to initial temperature—SEM and ESEM characterization

M. Mouret, A. Bascoul *, G. Escadeillas

Department Génie-Civil, LMDC, INSA–UPS, avenue de Rangueil, 31077 Toulouse Cedex, France

Manuscript received 30 July 1998; accepted manuscript 17 September 1998

Abstract

Both high initial and subsequent curing temperatures of concrete are known to induce decreases in strengths at 28 days of age. This paper deals with observation of the concrete microstructure to point out some differences that would be responsible for these changes in strength. For this purpose, conventional electron microscopy (SEM) and environmental electron microscopy (ESEM) techniques were used to study the microstructural features of normal strength concrete prepared at two initial temperatures (20°C and 50°C) and cured at either 20°C or 35°C. Using either SEM or ESEM, three major results can be observed on fracture surfaces. When initial temperatures are increased, the bulk paste seems amorphous, with a local poorly textured morphology. Moreover, air voids and capillaries can be seen close to the paste-aggregate interface. High initial temperatures also promote crystallization. Particularly, intermingling of little ettringite rods and large crystals of calcium hydroxide are observed on aggregate imprints, which results in an open microstructure of the paste. This latter observation explains the decrease in concrete strength as a result of a weakening of the interfacial transition zone. There are also outstanding differences between SEM and ESEM observations, which indicate artifacts of drying when using SEM.

Keywords: Microstructure; SEM; Curing; Ettringite; Interfacial transition zone

The strengths of concrete cast in summer, when the mix has a high initial temperature, may be lower than those expected from theoretical formulations. A previous study confirmed this and highlighted decreases in 28-day compressive strength and 28-day splitting tensile strength of laboratory concretes prepared with both heated aggregates and cement [1]. Particularly, the aggregate temperature rise from 20°C to 70°C implied an increase in the water demand of the concrete mixes. However, this alone cannot explain the drops in strength. Therefore, an explanation for this phenomenon was sought through an investigation of the microstructure.

Some earlier works dealt with the characterization and observation of the microstructure of cement-based materials cured at high temperatures. For cement pastes, Kjellsen et al. [2] showed, by observations on polished sections using a scanning electron microscope (SEM, BSEI mode), a more compact morphology of calcium hydroxide (CH) crystals when the curing temperature is increased and more systematic apparent hydration shells around the cement grains at 50°C than at 20°C, thus indicating a more densified inner product phase near the remnants of anhydrous material than in the interstitial space. In parallel, drops in compressive strength of companion mortar specimens cured at 50°C were noted. These statements pointed out the non homogeneous distribution of hydration products throughout the matrix when the curing temperature is increased. These results are in accordance with previous works showing, by indirect evidence, that a high rate of reaction due to increased curing temperature does not provide enough time for diffusion and uniform precipitation of hydration products throughout the interstitial space between the cement grains [3].

For mature concrete, conflicting data are found in the literature with regard to qualitative observations using either optical microscopy or electron microscopy. Patel et al. [4] showed that concrete subjected to curing temperatures between 20°C and 46°C kept a similar microstructure, with a limited coarsening at 46°C. In addition, they noted that 46°C curing temperature involved occasional concentrations of large crystals of CH at the paste-aggregate interface, and that this feature was more striking for concrete cured at higher temperatures (80°C) than at 46°C. In contrast, by studying different types of concrete made up of various aggregates and subjected to similar curing regimens (80–100°C), Clark et al. [5] assert that the higher the curing temperature, the lower will be the amount of CH at the paste-aggregate interface.

* Corresponding author. Tel.: 33-6155-9867; Fax: 33-6155-6265.

0008-8846/99/$–see front matter
PII: S0008-8846(98)00160-4

This paper is a part of a wide study dealing with the drops in 28-day strengths of manufacturing control concrete specimens produced in summer conditions and, generally speaking, in hot weather. It presents observations of fracture surfaces conducted under either SEM or environmental scanning electron microscope (ESEM). This present work has two objectives. First, it aims to show the effect of both initial temperature and curing temperature on the microstructure of concrete. Second, it tries to interpret typical SEM observations by comparing them with those of ESEM.

1. Experimental

1.1. Experimental programme

The study was conducted on normal-strength concrete specimens (28-day nominal strength of 35 MPa) composed of siliceous gravels. Cylinders (11 × 22 cm) were prepared with two different temperature formulae of constituent: 20°C (water)–20°C (aggregate)–20°C (cement) called 20–20–20 concrete, and 20°C (water)–70°C (aggregate)–70°C (cement) called 20–70–70 concrete, so that the initial temperatures of the mixes were 20°C and 50°C respectively. The same slump was required whatever the initial temperature. Additions of water were necessary for 20–70–70 concrete. The specimens were sealed and either cured under controlled laboratory conditions (20°C) for 1 day (cure 1) or conditions of hot weather (cure 2). Cure 2 simulated a time elapsed between placing and transporting the specimens to the control office: 35°C during the first 5 h after casting, next progressive decrease in temperature down to approximately 25°C until 24 h after mixing. After 1 day, all the specimens were removed from the molds and stored in water at 20°C up to the time of tests. Details of the materials, mix proportions, and mixing and testing procedures were described previously [1]. The cement used here is somewhat different from those used previously. It is a standard OPC CEM I 42.5 R (corresponding to ASTM type I) with a higher alkali content (1.4% by weight equivalent Na_2O). The chemical composition of the cement is reviewed in Table 1.

1.2. Specimen preparation

The cylinders were cured for 28 days. Next, fracture surfaces were taken from concrete cylinders that previously had been subjected to the splitting tensile test.

The specimens used for examination under the SEM (JEOL 35CF) by secondary electron imaging (SEI) were placed directly in an evaporator and maintained under high vacuum overnight. They were coated with carbon just before the observations were made.

Table 1
Chemical composition of the cement (percent by weight)

SiO_2 t	Al_2O_3	Fe_2O_3	CaO t	MgO	SO_3	K_2O	Na_2O	Cl	L.O.I.
19.20	5.55	2.88	62.6	2.39	3.37	1.48	0.49	0.02	1.50

Table 2
28-day compressive tests results

	Cure 1		Cure 2	
	Average (MPa)	SD (MPa)	Average (MPa)	SD (MPa)
20–20–20	39.2	0.8	35.7	0.6
20–70–70	33.0	1.1	31.9	1.0

Averages are given as means of six values.

The specimens examined under the ESEM (ELECTROSCAN fitted with dispersive energy X-ray spectrometer) using secondary electron mode were placed directly in the microscope chamber. Sample coating is not needed with this type of microscope. The fracture surfaces were observed at 6 torr of water pressure (10^6 times higher than in SEM) and at 20°C, implying an approximately 35% relative humidity. To achieve a high relative humidity close to 100%, water was sprayed in the specimen chamber. In this way, specimens were prevented from drying and no change in weight was measured. Moreover, these conditions allowed us to observe fracture surfaces larger than those examined in the SEM. As no drying occurs in ESEM, specimens observed are representative of the actual material. Therefore, it is worthwhile to compare the microstructural features of concretes observed by these two electron microscopic techniques. More details concerning the principles and functions of the ESEM are given by Danilatos [6].

2. Results

2.1. The 28-day compressive tests

The 28-day average compressive strength is reduced by as much as 16% and 11% for cure 1 and cure 2, respectively (relative variation of the mean value). A 19% reduction is noted between 20–20–20 concrete subjected to cure 1 and 20–70–70 concrete subjected to cure 2. These results (Table 2) are consistent with those described previously [1].

2.2. Fracture surfaces: SEM and ESEM observations

2.2.1. 20–20–20 concrete

2.2.1.1. Bulk cement paste. Disregarding the curing regimen, the matrix is generally compact and tends to be more amorphous than crystallized. Using qualitative energy dispersive X-ray analysis, the paste is found to be essentially composed of CSH gel classifiable as type III (Fig. 1A).

More pores and entrapped air voids are observed for cure 2 than for cure 1. When visible, they range in size from 10 to 120 μm. Within them, the paste presents features similar to the bulk one, and energy dispersive X-ray analysis shows that the hydrates essentially contain calcium and silicium. Sometimes, massive crystals of calcium hydroxide (CH) are visible, growing perpendicular to the void surfaces.

SEM observation shows that the paste is more microcracked than the that observed in ESEM, indicating that it is an artifact of drying (Fig. 1B).

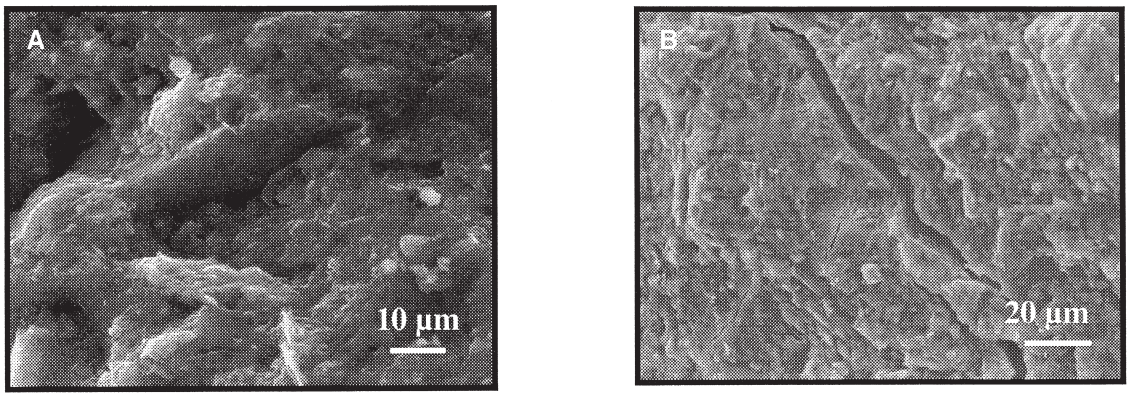

Fig. 1. Bulk cement paste (28-day old 20–20–20 concrete, cure 1, SEI). (*A*) ESEM; (*B*) SEM.

Very locally, the paste seems to have a less dense structure for cure 2 than for cure 1. In this case, the paste remains amorphous and hollow shells are apparent. This is noted by both SEM and ESEM examinations.

2.2.1.2. Cement-paste/aggregate interface. The hydration products formed near aggregates are not very different from those existing in the bulk matrix. Nevertheless, the textural appearance of the paste in the neighborhood of aggregates seems to be more porous for cure 2 than for cure 1. More CH crystals or pseudocrystals are seen near the edges of aggregates for cure 2 than for cure 1. When visible, these crystals run with different orientations to the interface, with their basal plane approximately either parallel (C-axis perpendicular) or perpendicular (C-axis parallel) to the surface of aggregates. The crystals are 10 to 15 μm in size, disregarding the curing temperature. They partially surround the aggregates, thus indicating a possible localized bleeding. Fig. 2A illustrates these observations by ESEM; Fig. 2B is representative of SEM examinations.

ESEM technique shows good bond between the paste and the aggregate, so sometimes it is difficult to distinguish the interface. This suggests that, using SEM, drying generated before coating and, next, during the observations of the specimens either creates microcracks or involves the widening of pre-existing ones along the interface. Therefore, the gap existing at the paste-aggregate interface revealed by SEM observations leads us to believe that the bond between paste and aggregate would be weaker than the paste itself in the vicinity of the interfacial transition zone (ITZ).

SEM and ESEM observation of the imprints of the aggregates shows the same typical morphology of the paste-facing surface (Fig. 3):

- First, a 5- to 10-μm thick film of CH,
- Second, small granulated formations that are not crystallized and which are composed of calcium, silicon, sulfur, and traces of aluminum, potassium, and iron (Fig. 3). This configuration results in a highly porous paste. Sometimes, the paste is composed of CH crystals perpendicular to the aggregate imprint and these granulated formations.

Regardless of the curing temperature at early ages, these observations are typical of ESEM. However, using SEM, some differences may exist. Indeed, examinations of areas where aggregate has broken away show either local developed crystallizations (CSH particles, perpendicular CH crystals [Fig. 4A], AFt rods that are more apparent and more developed for cure 2 than for cure 1 [Fig. 4B], or

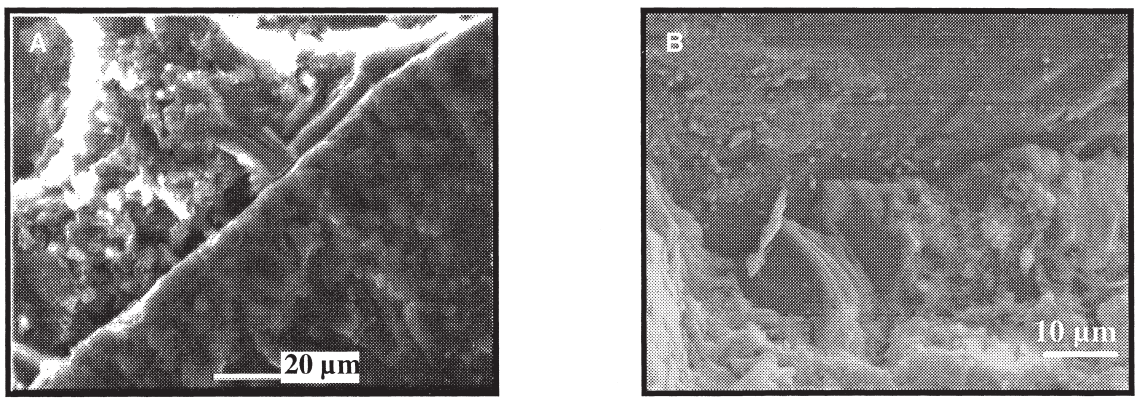

Fig. 2. Paste-aggregate interface (28-day old 20–20–20 concrete, cure 2, SEI). (*A*) ESEM; (*B*) SEM.

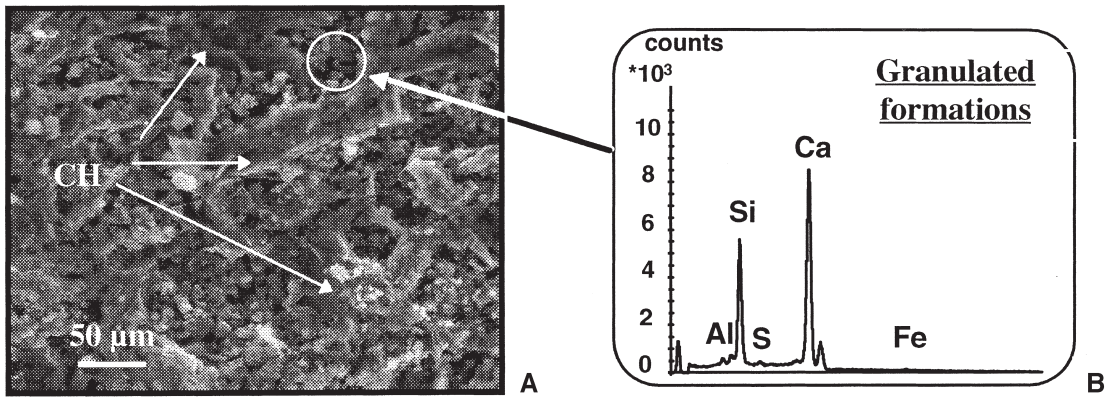

Fig. 3. Area of imprint surface left by lost aggregate (28-day old 20–20–20 concrete, cure 1, ESEM-SEI).

dense microstructures as a result of an intimate intermingling of amorphous CH and CSH gel [Fig. 4C]).

Sometimes, air voids are visible in the vicinity of the paste-aggregate interface or on aggregate imprints; their characteristics are the same as those observed in the bulk paste. Capillary pores and hollow-shell grains are more visible on the imprint surface of an aggregate that has broken away than within the bulk matrix. This is certainly due to an increase in the local water-to-cement ratio in these regions. The systematic presence of hollow grains has been noted previously [7].

2.2.2. 20–70–70 concrete

2.2.2.1. Bulk cement paste. Whatever the curing temperature at early ages, most often it seems that there is no particular crystallization. However, the paste can be occasionally not very dense, and typical small calcium silicate crystals are visible locally (Fig. 5). This feature is more significant

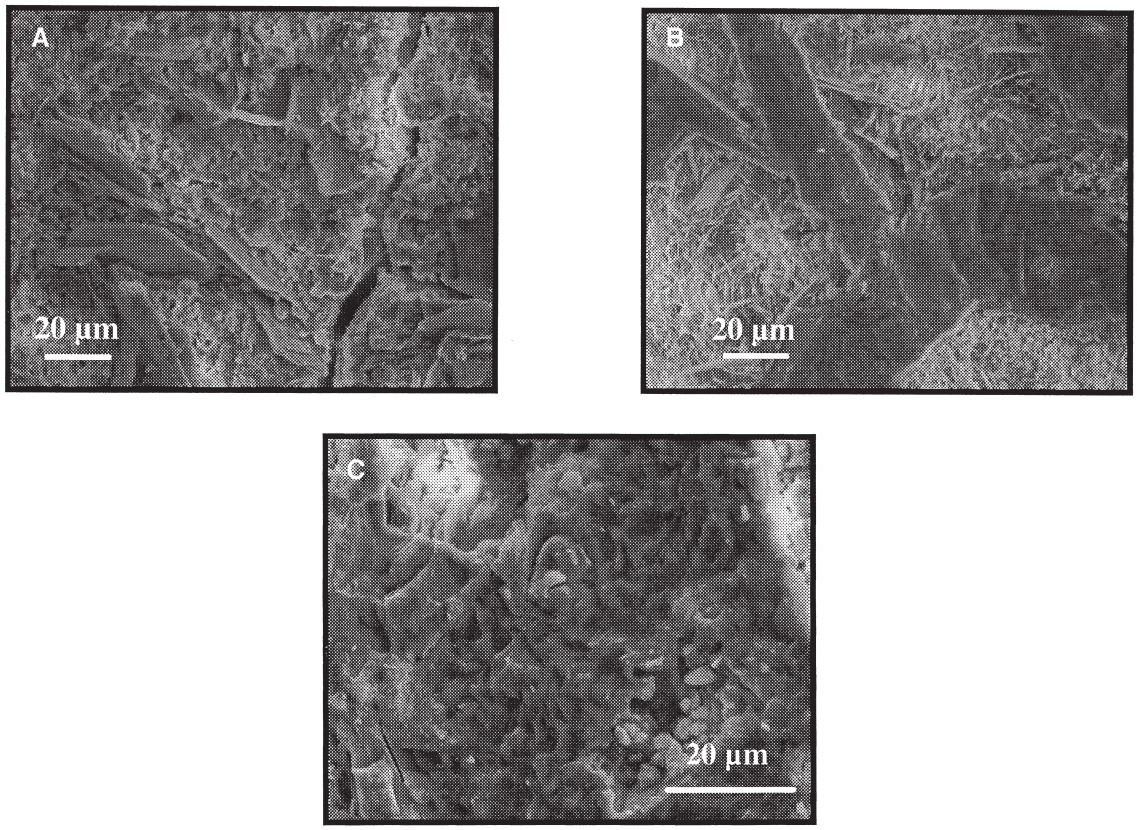

Fig. 4. Imprint surface left by lost aggregate (28-day old 20–20–20 concrete, SEM-SEI). (*A*) Cure 1; (*B*) cure 2; (*C*) cure 1.

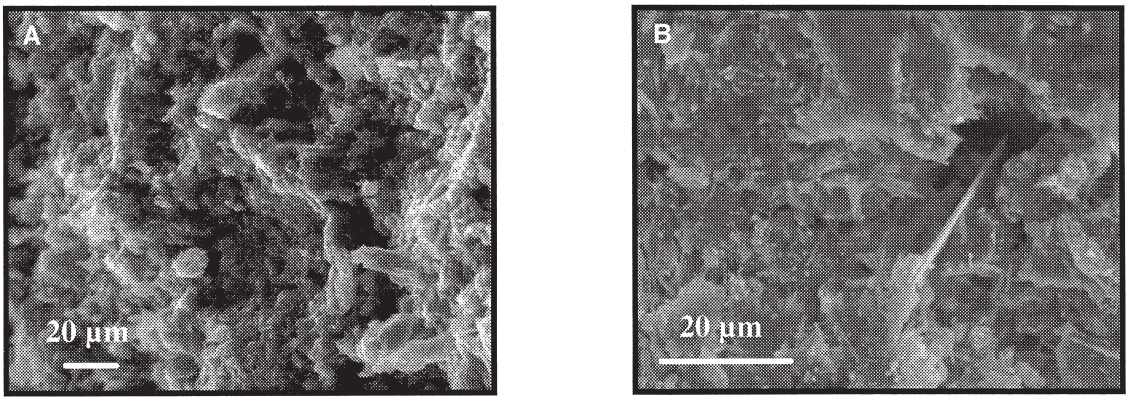

Fig. 5. Morphology of bulk cement paste (28-day old 20–70–70 concrete, cure 2, SEI). (*A*) ESEM; (*B*) SEM.

for cure 2 than for cure 1. Moreover, a large number of capillaries and entrapped air voids with sizes up to 350 μm are observed. In other respects, the occurrence of hollow-shell grains is the same here as in the bulk paste of 20–20–20 concrete.

2.2.2.2. Paste-aggregate interface. Concerning the interfaces of 20–70–70 concrete, the following can be noted:

- A 5- to 10-μm thick film of CH (Fig. 6) on aggregate imprints,
- In the case of cure 1, small granulated formations behind the CH surface layer (Fig. 6) (the composition of these particles is the same as described for Fig. 3),
- Well-oriented CH crystals with their C-axis parallel to the interface, as indicated by the arrows in Fig. 7.
- In the case of cure 2, ettringite rods and massive CH crystals often observed by SEM and ESEM (Fig. 8) on areas where aggregates have broken away and behind the CH layer.

3. Discussion

3.1. Comparison between SEM and ESEM techniques

Whatever the temperature conditions, SEM observation shows a local crystallization (see Fig. 4). This leads us to believe that the sample preparation could locally modify the microstructure of concrete. In other words, the crystalline morphology could be a result of drying for SEM preparation and observation. Indeed, within the fresh mix, water-rich zones exist near aggregates that probably are the consequence of bleeding channels. Consequently, water can move and dissolve species, which then will precipitate and form first an amorphous CH layer and second microcrystals, namely, granulated formations. Draining off the residual water when drying the samples for SEM observation could emphasize this phenomenon and intensify the crystallization, like the one of ettringite rods (Fig. 4B). This is consistent with the finding that these granulated formations are partially composed of sulfur and aluminum (Fig. 3).

3.2. Comparison between 20–20–20 concrete and 20–70–70 concrete

3.2.1. Bulk cement paste

The bulk paste of 20–70–70 concrete seems to be locally less compact than that of 20–20–20 concrete even less with cure 2 than with cure 1. Such a morphology can be explained by the fact that high temperature makes the dissolved cement components difficult to move. Indeed, high temperature rapidly increases the occurrence of topochemical reactions to the detriment of through solution mechanisms. Consequently, the hydration products are not evenly

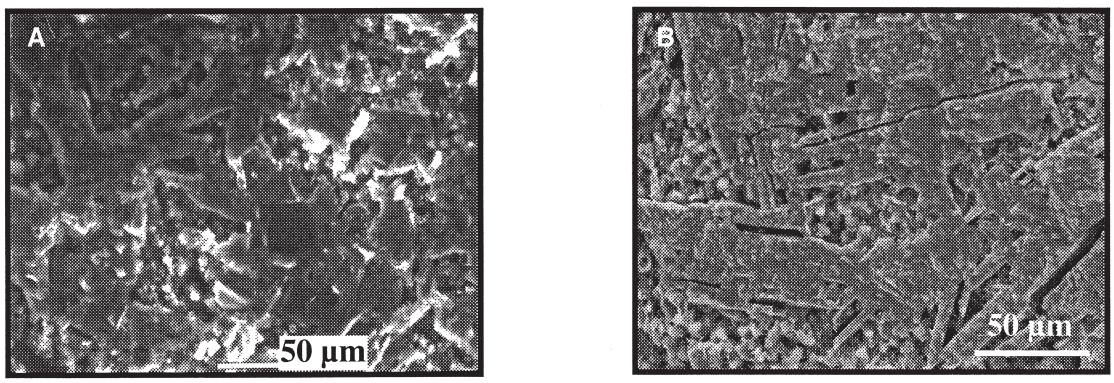

Fig. 6. Imprint surface left by lost aggregate (28-day old 20–70–70 concrete, cure 1, SEI). (*A*) ESEM; (*B*) SEM.

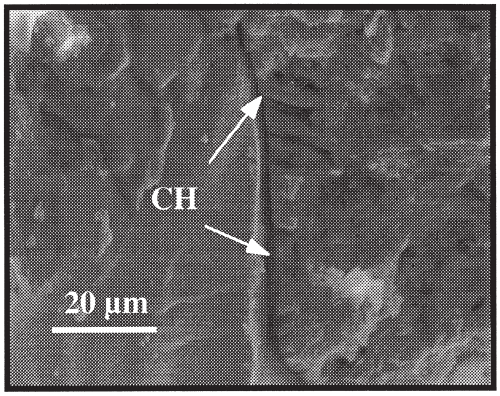

Fig. 7. CH crystals growing close to the surface of a sand grain with perpendicular orientation (28-day old 20–70–70 concrete, cure 1, SEI).

distributed. This phenomenon was previously identified [3] and recently discussed [8]. However, in the present study, this localized morphology cannot be a major reason for the drops in strength.

3.2.2. Paste-aggregate interfaces

Some differences between 20–20–20 concrete and 20–70–70 concrete are obvious. CH can be systematically observed in 20–70–70 concrete, more visible for cure 2 than for cure 1. This was confirmed by the observation of flat polished sections in the SEM. Two morphologies of CH exist as as follows:

- The surface layer visible on aggregate imprints (Fig. 6) indicates that a weak bond exists between aggregates and cement paste when the temperature is increased. This is consistent with the drops in splitting tensile strengths as described previously [1] when both initial concrete temperature and curing temperature are high.
- Oriented CH crystals at the interfacial zone make the microcrack growth easier along their cleavage surfaces. This is an another reason for explaining the "weak link" structure of the paste-aggregate interface of concrete prepared and cured at high temperatures.

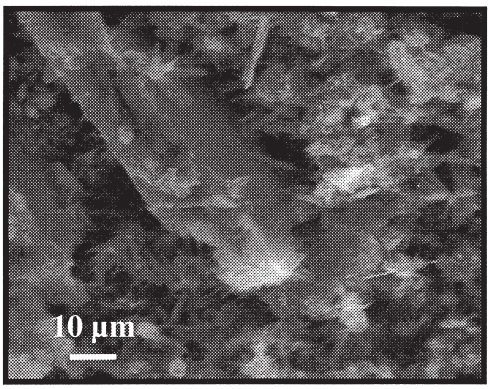

Fig. 8. Developed crystallization on aggregate imprint (28-day old 20–70–70 concrete, cure 2, ESEM-SEI).

Besides, developed AFt rods and large crystals of CH observed on aggregate imprints of 20–70–70 concrete subjected to cure 2 make the paste more porous than that of 20–20–20 concrete. This induces drops in concrete strength.

All these features help to explain the drops in strength as the result of the weakening of the ITZ.

To some extent, it is possible to clarify the systematic presence of CH in 20–70–70 concrete compared with 20–20–20 concrete. As noted by many authors [9], a high initial concrete temperature leads to an increase in the water demand [1]. This elevated temperature of the concrete mix implies water-rich zones near the aggregate that also are rich in dissolved species. In addition, a subsequent high curing temperature accentuates and extends the first heating effect. Consequently, an easier lime precipitation occurs close to the aggregate, because lime solubility is decreased when temperature is increased [10].

Finally, recalling the conflicting data noted in the introduction, it seems that the investigations of Patel et al. [4] are in agreement with the results of the present study.

4. Conclusions

The effect of both high initial and subsequent curing temperatures on the microstructure of normal strength concrete was examined. By using either SEM or ESEM, we can conclude by pointing to some major features related to the initial conditions of concrete.

- When initial concrete temperatures are increased from 20°C to 50°C, the bulk paste very often seems amorphous, with a poorly textured morphology in places. The same remarks can be made when curing temperature at early ages is increased from 20°C to 35°C. Air voids and capillaries also are more visible at these high temperatures than at low temperatures, notably near the paste-aggregate interface.
- In the vicinity of the aggregate, the paste is more porous with both high initial and subsequent curing temperatures than with low temperatures. Indeed, an open microstructure of the paste is observed on aggregate imprints: it is composed of ettringite rods and intergrown massive calcium hydroxide (CH) crystals.
- For high initial temperature conditions, CH crystals are observed systematically at the paste-aggregate interfaces. They are oriented with their C-axis either parallel or perpendicular to the interface.

All these features can explain decreases in strength related to elevated temperatures as a result of a weakening of the ITZ.

By comparing SEM and ESEM pictures of the same concrete, several differences must be emphasized, whatever the temperature.

- With SEM, the bulk paste seems more microcracked than with ESEM. This results from the drying during preparation and observation. Instead of the close proximity between paste and aggregate observed under ESEM, a gap between the paste and the aggregate is visible under SEM. This difference is due to the drying shrinkage. It shows that the bond strength between paste and aggregate is weaker than that of the paste itself at the ITZ.
- Even if the initial temperature of concrete and the subsequent curing temperature are low, SEM observation shows locally developed crystallization in areas where both the aggregate and the CH surface layer have broken away. Drying is partially responsible for this phenomenon, which is not observed for the same concrete, when using ESEM.

Acknowledgments

The authors wish to acknowledge the Association Technique de l'Industrie des Liants Hydrauliques (ATILH) for supporting this research.

References

[1] M. Mouret, A. Bascoul, G. Escadeillas, Cem Conc Res 27 (1997) 345.
[2] K.O. Kjellsen, R.J. Detwiler, O.E. Gjørv, Cem Conc Res 21 (1991) 179.
[3] G.J. Verbeck, R.H. Helmuth, Structures and physical properties of cement pastes, Proceedings of the Fifth International Symposium on the Chemistry of Cement, Session III-1, Tokyo, Japan, 1968, pp. 1–32.
[4] H.H. Patel, C.H. Bland, A.B. Poole, Cem Conc Res 25 (1995) 485.
[5] B.A. Clark, E.A. Draper, R.J. Lee, J. Skalny, M. Ben-Bassat, A. Bentur, Electron-optical evaluation of concrete cured at elevated temperatures, Proceedings of the International Symposium on How to Produce Durable Concrete in Hot Climates, ACI Committee 201, San Juan, 1992, pp. 41–60.
[6] G.D. Danilatos, Foundations of environmental microscopy, in: P.W. Hawkes (Ed.), Advances in Electronics and Electron-Physics, Academic Press, Boston, 1988, pp. 71–109.
[7] S. Diamond, The microstructure of cement paste in concrete, Proceedings of the Eighth International Congress on the Chemistry of Cement, Rio de Janeiro, Brasil, 1986, p. 122.
[8] K.O. Kjellsen, R.J. Detwiler, Cem Conc Res 22 (1992) 112.
[9] ACI Committee 305, ACI Mater J 88 (1991) 417.
[10] K.L. Scrivener, W. Wieker, Advances in hydration of cements at low, ambient and elevated temperatures, Proceedings of the Ninth International Congress on the Chemistry of Cement, New Dehli, India, 1992, p. 449.